



PERGAMON

Pattern Recognition 32 (1999) 1911–1922

**PATTERN  
RECOGNITION**

THE JOURNAL OF THE PATTERN RECOGNITION SOCIETY

# Use the Fuzzy Hough transform towards reduction of the precision/uncertainty duality

Olivier Strauss\*

*Laboratoire d'Informatique de Robotique et de Micro-électronique de Montpellier, Department of Robotics, Université Montpellier II, 161 rue Ada, 34392 Montpellier, France*

Received 5 November 1998; received in revised form 7 December 1998; accepted 7 December 1998

## Abstract

The Hough transform is a popular method for detecting complex forms in digital images. However, the technique is not very robust since several parameters that determine the scope of the detection results, such as quantization thresholds and intervals, must first be defined. In the present paper, we propose to enhance shape detection with the Hough transform through fuzzy analysis. One chief drawback of the Hough transform, i.e., the uncertainty/precision duality, is thus reduced. © 1999 Pattern Recognition Society. Published by Elsevier Science Ltd. All rights reserved.

*Keywords:* Hough transform; Fuzzy subsets; Uncertainty; Precision; Quantization

## 1. Introduction

The Hough transform (HT) was first introduced in the 1960s as a method for detecting sets of collinear points in binary noisy digital images [1]. It was brought to the attention of the scientific community through the works of Rosenfeld [2] and Duda and Hart [3].

This technique was later extended to the detection of arbitrary shapes [4] in arbitrary dimensioned spaces. Hough-like transforms have also been suggested for pattern recognition [5].

There have been several proposals to reduce the huge memory storage capacity and computational time required for HT, a substantial drawback of this technique [6,7].

Many papers have focused on the effects of errors due to random noise and data quantization. Probabilistic analysis of the HT process seems particularly complex and suggested solutions are still highly empirical. A powerful approach has been proposed in Ref. [8] to

design a tool to analyze HT performance by using hypothesis testing methods.

The Hough transform and its extensions have been reviewed in detail [9,10] and an exhaustive bibliography is available [11,12]. Comparisons between probabilistic and non-probabilistic approaches are reviewed in Ref. [13].

Despite the abundance of papers dedicated to HT, relatively little attention has been paid to what we termed *the uncertainty/precision duality*. This duality could be set out as follows: as the shape detection precision increases, the reliability of the detection decreases. This seems to be due to the binary aspect of the vote in the classical Hough transform (CHT).

Han et al. [14] proposed using fuzzy subset theory to deal with the problem of approximate concepts in HT. They designed a fuzzy Hough transform (FHT) which generalized the distributed voting principle described by Thrift and Dunn [15]. However, this method makes no distinction between data uncertainty and expected or computationally induced parameter uncertainty. In addition, there is no benefit to assessing the data in terms of confidence.

Our new FHT approach takes current knowledge on uncertainty into consideration to improve shape detection.

\*Tel.: + 33-467-418-587; fax: + 33-467-418-500.

E-mail address: Olivier.strauss@lirimm.fr (O. Strauss)

The present paper is organized as follows. Section 2 includes a short survey of CHT to outline some notation points and specify how the transform is conventionally computed. Section 3 provides a brief introduction to fuzzy subset theory. FHT is presented in Section 4 as a *fuzzification* of CHT. We demonstrate that this new formulation is helpful for solving problems such as thresholding, peak enhancement, quantization of parameter space and data localization uncertainty. It allows the user to deal separately with data uncertainty, data confidence, parameter uncertainty and parameter confidence. This new formulation is highlighted through a few examples given in Section 5, with CHT and FHT compared according to their abilities to identify approximate straight lines in a particularly noisy image. Discussion, conclusions and extensions are proposed in Section 6.

The study was restricted to the detection of straight lines in images in order to simplify the statement of the method.

## 2. Classical Hough transform

### 2.1. Evidence gathering procedure

A brief overview of CHT is presented, but we only consider a context in which the domain is a bounded box of  $\mathbb{R}^2$  points, i.e., a conventional image.

Each pixel in image  $I$  is represented by its coordinates  $(i, j)$  that map real positions  $(x_i, y_j)$  in the image. Let us assume that in this image we look for a set of curves defined by the function  $f(x, y, P) = 0$ , where vector  $P$  of size  $n$  is the parameter.

If we consider that  $E$  represents a bounded subset of image points that are assumed to belong to one of the sought-after curvatures, then at  $E$  the *Hough transform* maps a function  $\mathcal{H}$  defined on  $\mathbb{R}^n$ .

Many Hough transforms have been described in the literature, all of them are highly combinational. The *1-to-m Hough transform* [9] is the most computationally efficient version, and involves mapping a number of  $E$  points to each  $P$  point in the parameter space, such that  $f(x, y, P) = 0$ .  $\mathcal{H}$  acts as a counter function and the array it produces is called an accumulator array. Image curves in the parameter space are characterized by peaks in the  $\mathcal{H}$  function.

It would not be beneficial to assess the  $\mathcal{H}$  function for the entire  $\mathbb{R}^n$  space given that the image is a bounded subset. Therefore,  $\mathcal{H}$  is evaluated on a bounded subset  $\Omega$  of  $\mathbb{R}^n$ , since the boundaries of this subset can be directly deduced from the image boundary by the function  $f$ .

For practical purposes, the parameter space is subdivided into a number of cells in the subset  $\Omega$ . Otherwise, evaluation of  $\mathcal{H}$  within an infinite number of  $\Omega$  points would give rise to several problems, including complex calculations.

Using the 1-to- $m$  Hough transform to map a cell  $\Pi$  of  $\Omega$  involves calculating the cardinal number of the subset  $E_\pi$  for all the points of  $E$  that “obviously” belong to any of the forms that arise from the box  $\Pi$  and the function  $f$ . This is given by  $(x, y)_E$ , such that:

$$(x, y) \in E_\pi \Leftrightarrow \exists P \in \Pi / f(x, y, P) = 0. \tag{1}$$

Eq. (1) clearly demonstrates that  $(x, y)$  belongs to the subset  $E_\pi$  and also that

$$\begin{aligned} \mathcal{H}(\Pi) &= \sum_{(x, y) \in E} \sum_{P \in \Pi} \zeta(f(x, y, P)) = \sum_{(x, y) \in E} \chi_{E_\pi}(x, y) \\ &= \sum_{(x, y) \in E} \text{MIN}(\chi_E(x, y), \chi_{E_\pi}(x, y)) \end{aligned}$$

with  $\zeta(u \neq 0) = 0$  and  $\zeta(0) = 1$ .  $\chi_E$  is the characteristic function of  $E$  subset.

We limited the present study to the detection of straight lines in an image to simplify statement of the method.

### 2.2. Detection of straight lines in an image

Since the studies of Duda and Hart [3], it is a common practice to define the membership of a point  $(x, y)$  in the plane to a straight line by the following relation:

$$f(x, y, \rho, \theta) = \rho - x \cos \theta - y \sin \theta = 0$$

$$\text{with } (\rho, \theta) \in \mathbb{R} \times [0, \pi],$$

where  $\theta$  represents the orientation of the vector normal to the line, and  $\rho$  denotes the distance from the straight line to the origin.

Polar representation of a straight line (Fig. 1) is doubly useful because it is homogeneous and facilitates definition of a bounded variation space  $\Omega$ . The space  $\Omega$  is subdivided into the same-sized cells  $(2\delta\rho \times 2\delta\theta)$ , such that

$$[\rho_p - \delta\rho, \rho_p + \delta\rho] \times [\theta_q - \delta\theta, \theta_q + \delta\theta] = P_p \times \Theta_q.$$

Except for a few exceptions described later, the *1-to-m* Hough transform is used to analyze each cell as follows: for each point  $(x_i, y_j)$  of  $E$ , and for each  $\theta_q$ , the distance  $\rho$  from the straight line to the origin is simply determined by

$$\rho = x_i \cos \theta_q + y_j \sin \theta_q.$$

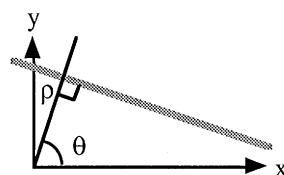


Fig. 1. Polar representation of a straight line.

The accumulator function  $h$  is then incremented in the cell  $(P_p \times \Theta_q)$  such that  $\rho \in [\rho_p - \delta\rho, \rho_p + \delta\rho]$ . Now that this formulation is stated, several further questions arise:

- How can the subset  $E$  be extracted from the image points that theoretically belong to a straight line?
- Are the detection features of the transform affected by the size of the cells in the parameter space? If so, can an optimal size be defined?
- How can peaks in the transform array be detected? Can this detection be assessed for confidence?
- How precise is the transform in detecting straight lines? Can this precision be enhanced?

In Section 4, we demonstrate that these questions can be neatly answered by fuzzy subset theory. This theory is briefly outlined in Section 3.

### 3. An update on the fuzzy concept

Some of the tenets of fuzzy subset theory are now reviewed to set the stage for the discussion that follows. Further details on fuzzy subsets are given in [16,17].

#### 3.1. Fuzzy intervals

Fuzzy subsets of  $\mathcal{R}$  are called *fuzzy quantities*.

A fuzzy interval  $Q$  is a fuzzy convex quantity, which means that the membership function is quasi-concave:

$$\left. \begin{array}{l} \forall (u, v) \in \mathbb{R}^2 \\ \forall w \in [u, v] \end{array} \right\} \mu_Q(w) \geq \text{MIN}(\mu_Q(u), \mu_Q(v)).$$

A fuzzy quantity  $Q$  can also be considered as a fuzzy interval if all of its  $\alpha$ -cuts are crisp intervals. Moreover, if the fuzzy interval support is bounded, then the fuzzy interval itself is bounded. Fuzzy intervals (Fig. 2) can generally be conveniently denoted using an LR representation [17]. A fuzzy interval can thus be fully characterized by its kernel and support.

Finally, a generalization of the Cartesian product notion can be defined. If we consider  $Q_1$  and  $Q_2$  as two fuzzy intervals characterized by their membership functions  $\mu_1$  and  $\mu_2$ , then the *fuzzy box*  $Q_1 \times Q_2$ , the Cartesian

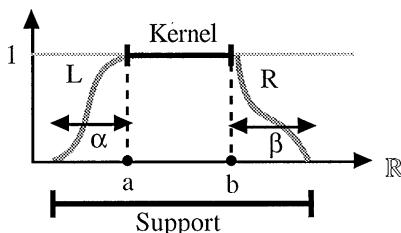


Fig. 2. LR-type fuzzy interval.

product of  $Q_1$  and  $Q_2$ , is denoted by  $\mu_{Q_1 \times Q_2}$ , such that  $\mu_{Q_1 \times Q_2}(x_1, x_2) = \text{MIN}(\mu_1(x_1), \mu_2(x_2))$ .

#### 3.2. Extension principle

In this section, we present a generalization of the extension principle as applied to error calculus.

The extension principle addresses the following problem. Let  $f$  be a function of  $N$  fuzzy variables  $x_n$ . The variation domain of  $x_n$  is the fuzzy subset characterized by its membership function  $\mu_n(x)$ . Using the extension principle, we can define the variation domain of the variable  $y$  where  $y = f(x_1, \dots, x_N)$ .

Assuming that  $x_n$  variables are non-interactive (i.e., if the variation domain of variable  $x_i$  does not depend on the values of the other variables  $x_j$  for all pairs  $(i, j)_{i \neq j}$ ), then the variation domain of  $y$  is defined by  $\mu_f(y)$ , such that

$$\mu_f(y) = \text{SUP}_{x_1, \dots, x_N} \{ \text{MIN}(\mu_1(x_1), \dots, \mu_N(x_N)) / f(x_1, \dots, x_N) = y \}.$$

Assuming that the variation domain of each  $x_n$  is an LR-type fuzzy interval  $X_n$ , then the variation domain of  $(x_1, \dots, x_N)$  is a fuzzy box  $X$  of  $\mathbb{R}^N$ , the Cartesian product of  $N$  fuzzy intervals  $X_n$ .

In the light of a few reasonable hypotheses on the size of box  $X$ , the variation domain of  $y$  can be estimated by an LR-type fuzzy interval. Since it is not always possible to precisely calculate  $\mu_f$ , we obtain  $a_y, b_y, \alpha_y$  and  $\beta_y$  which define  $\bar{\mu}_f$  an approximation of  $\mu_f$  via a limited first-order development of  $f$  [17].

$$a_y = f(a_1, \dots, a_N),$$

$$\alpha_y = \frac{\partial f}{\partial x_1}(a_1, \dots, a_N)\alpha_1 + \dots + \frac{\partial f}{\partial x_N}(a_1, \dots, a_N)\alpha_N,$$

$$b_y = f(b_1, \dots, b_N),$$

$$\beta_y = \frac{\partial f}{\partial x_1}(b_1, \dots, b_N)\beta_1 + \dots + \frac{\partial f}{\partial x_N}(b_1, \dots, b_N)\beta_N.$$

We often use the notational misnomer  $f(X)$  to denote the fuzzy subset defined by the function  $f$  and the fuzzy subset  $X$ .

### 4. Fuzzy Hough transform

The Hough transform will now be analyzed according to fuzzy subset theory.

#### 4.1. Thresholding

Users of the HT first have to face the problem of defining the subset  $E$  of image points that supposedly belong to the sought-after straight lines.

### 4.1.1. Binary thresholding

Image pixels can generally be separated into two subsets  $E$  and  $\bar{E}$  according to grey level, gradient and curvature properties.  $E$  is the subset of points belonging to one of the sought-after straight lines, and its complement  $\bar{E}$  is the subset of points that do not belong to any straight line.

Automatic search algorithms for a grey-level threshold  $s$  that allows this separation are generally based on statistical signal separation properties [18].

There are no problems with such procedures when an optimal image, i.e., a clear, uniform and well-contrasted image, is analyzed.

When the image is suboptimal, the operator is obliged to over- or under-estimate the threshold. With an over-estimated threshold, many points belonging to sought-after forms are not taken into account. With an underestimated threshold, the  $E$  subset contains points that belong to none of the sought-after forms (background noise). In this case, many peaks appear in the HT which do not match any real straight lines in the image.

Many solutions have been proposed to overcome this problem, including that of Ref. [19], whereby grey-level values are used directly to weigh HT votes.

We use a similar technique to define  $E$  as a fuzzy subset of the original image. This calls for further details on threshold detection procedures.

### 4.1.2. Separation threshold detection

Two hypotheses can be put forward for each pixel  $(i, j)$ :

- the null hypothesis  $\mathcal{H}_0$ : “the pixel belongs to one of the sought-after lines” i.e.,  $(i, j) \in E$ ,
- the alternative hypothesis  $\mathcal{H}_1$ : “the pixel does not belong to one of the sought-after lines”, i.e.,  $(i, j) \in \bar{E}$ .

When looking for black lines on a white background, it is possible to determine whether  $(i, j)$  belongs to  $E$  or  $\bar{E}$  via the grey-level threshold  $s$ . The null hypothesis is accepted if  $ng(i, j) < s$ . Conversely, the alternative hypothesis is accepted if  $ng(i, j) > s$ .

Assuming that the grey levels of each pixel represent its probability of membership to  $E$  (or to  $\bar{E}$ ), two types of risk can be defined [20]

- the first  $\alpha$ -type, involving rejection of an  $E$  pixel when it actually belongs to  $E$ :  $\alpha = P(\text{reject } \mathcal{H}_0 / \text{real } \mathcal{H}_0)$ ,
- the second  $\beta$ -type, involving rejection of an  $\bar{E}$  pixel when it actually belongs to:  $\bar{E}$ :  $\beta = P(\text{reject } \mathcal{H}_1 / \text{real } \mathcal{H}_1)$ .

As  $s$  drops,  $\alpha$  decreases and  $\beta$  increases. Hence, establishing a threshold means finding a good trade-off between  $\alpha$  and  $\beta$  risks, or favoring one hypothesis over the other.

The results of this type of trade-off closely depend on the hypotheses put forward concerning the grey-level distribution in the image.

### 4.1.3. Fuzzy thresholding

In contrast, two thresholds  $s^+$  and  $s^-$  are readily defined by setting equivalent probability thresholds for each risk ( $\alpha = \beta$ ). Two subsets  $E_1 \subset E$  and  $E_2 \subset \bar{E}$  can thus be extracted from the image. Hence, with certainty,  $E_1$  represents points belonging to a line (risk < threshold), and  $E_2$  represents the set of points belonging to no line. The membership status of points with grey levels between these two thresholds is not as clearcut.

This vague membership situation is easily taken into account by considering  $E$  as a fuzzy subset. Hence,  $E$  contains all  $E_1$  points, no  $E_2$  points, and to various extents can contain points that do not belong to  $E_1$  or  $E_2$ .

$E_1$  and  $E_2$  can be considered as empty subsets without any loss of generality, which means that no image thresholds are defined.

When searching for black lines on a white background, the membership  $\mu_E(x_i, y_j)$  of a pixel  $(i, j)$  with a grey level  $ng(i, j)$  to a fuzzy subset  $E$  could be defined from a  $\mathcal{L}$ -function by

$$\begin{aligned} \mu_E(x_i, y_j) &= 1 && \text{if } ng(i, j) < s^-, \\ \mu_E(x_i, y_j) &= \mathcal{L}\left(\frac{ng(i, j) - s^-}{s^+ - s^-}\right) && \text{if } s^- < ng(i, j) < s^+, \\ \mu_E(x_i, y_j) &= 0 && \text{if } s^+ < ng(i, j). \end{aligned}$$

When  $I_{pq}$ , the crisp subset of  $I$ , is denoted by

$$I_{pq} = \{(x, y) \in I \mid |x \cos(\theta_q) + y \sin(\theta_q) - \rho_p| < \delta\rho\}$$

then, in assessing the  $P_p \times \Theta_q$  cell, the HT is equal to the fuzzy cardinal of the subset  $E \cap I_{pq} = E_{pq}$ .

$$\mathcal{H}(P_p \times \Theta_q) = \text{CARD}(E_{pq}) = \sum_{(x, y) \in I_{pq}} \mu_E(x, y).$$

In practice, when the image grey-level distribution is unknown, it is better to use a linear function:

$$\mathcal{L}(u) = 1 - u \quad \text{if } u \in [0, 1] \quad (\text{Fig. 3})$$

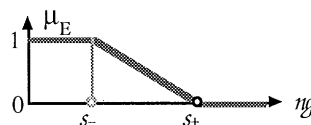


Fig. 3. Fuzzy thresholding.

However, if the image contrast is known, it can be taken into account by using *semantic modifiers* for membership of the subset to  $E$  [16].

### 4.2. Quantization

In practice, we noted that use of the HT subdivides  $\Omega$  into a certain number of cells. A counter is associated with each cell which indicates the number of image points that belong to any of the straight lines defined by this cell.

Many papers have rightly focused on the problem of quantization of  $\Omega$ .

There are two objectives in adjusting quantization:

- enhanced computation performance (less storage memory required, reduced computation time),
- enhanced algorithm performance (precision, confidence).

The first objective reduces the cell number (increased quantization), while the status of the second is not as clearcut, and is the focus of the present study.

#### 4.2.1. Imprecision/uncertainty

Although the aim is to increase line detection *precision*, quantization is clearly reduced. This reduction can also be motivated by a high density of lines in the image. In addition to a substantial increase in computation time, there will be a lower accumulator coefficient, thus increasing *uncertainty* in detecting each straight line. When this phenomenon is exaggerated with an excessive quantization, the accumulator array will only contain a maximum of one point per cell.

Conversely, if we intend to tolerate a poor fit between the model and reality, then it would be better to increase quantization. This increases the values of the accumulators associated with each cell, thus increasing the confidence that straight lines are present in the image. However, enhancing the *certainty* in the detection of each line will increase the *imprecision* of this detection.

The main reason for this dichotomy between the expected line detection precision and the certainty that the line is present in the image is the binary aspect of the vote in CHT.

Many authors have offered solutions to buffer the effects of this duality. They can be classified into five categories:

- *optimal* quantization [21],
- non-uniform quantization [22],
- multi-scale quantization [18],
- adaptive quantization [23],
- distribution of votes to neighboring cells [15].

The aim of the latter method is to account for the uncertainty of detecting characteristic points by incrementing the accumulators of all cells whose representative lines intersect the uncertainty zone (Fig. 4).

The fuzzy vote is associated with this technique, as described in Ref. [14]. The uncertainty zone attached to each characteristic point is represented by a fuzzy subset with a uniform isotropic membership function. In practice, the vote of each characteristic point is weighted according to the Euclidean distance that separates it from the ideal straight line represented by the cell.

This method is innovative but does not differentiate between imprecision in pixel detection (intrinsic to image

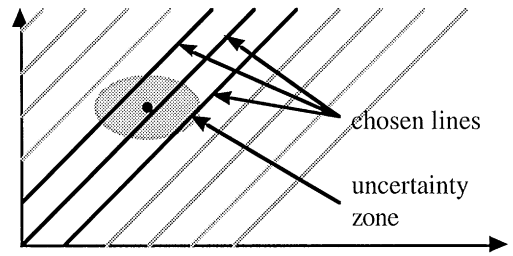


Fig. 4. Uncertainty in detecting a pixel.

sensors) and expected imprecision which is intrinsic to line detection objectives set by the operator.

Moreover, we believe that the hypothesis of an isotropic pixel membership function is unfounded and prefer to view the image as a fuzzy tiling<sup>1</sup> of  $\mathbb{R}^2$  points; the  $\Omega$  tiling is also considered as fuzzy.

#### 4.2.2. Distributed vote

In a classical Hough transform (CHT) [24], each pixel  $(i, j)$  is considered as an intersection point of coordinates  $(x_i, y_j)$  in the image  $I \subset \mathbb{R}^2$ . The parameter space is subdivided into  $(2\delta\rho, 2\delta\theta)$ -sized boxes  $P_p \times \Theta_q$  centered on  $(\rho_p, \theta_q)$ .

Each pixel  $(x_i, y_j)$  gives rise to a sine curvature in  $\Omega$  space. The Hough transform is assessed by incrementing, for each characteristic point (i.e.,  $(x_i, y_j) \in E$ ), accumulators associated with  $\Omega$  boxes that intersect the sine curvature in a non-null manner (Fig. 5).

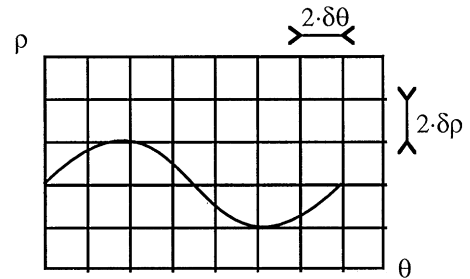


Fig. 5. Sine curvature fitted to an image point  $(x_i, y_j)$ .

In practice, this means calculating the  $\rho$  values matching each  $\theta_q$  value of  $\theta$ :  $\rho_p = (x_i \cos \theta_q + y_j \sin \theta_q)$  and incrementing the  $P_p \times \Theta_q$  cell accumulator, such that  $\rho \in [\rho_p - \delta\rho, \rho_p + \delta\rho]$ .

To account for uncertainty in detecting characteristic points, it is necessary to consider each pixel  $(i, j)$  as a  $(2\delta x, 2\delta y)$ -sized box  $X_i \times Y_j$  of the image  $I \subset \mathbb{R}^2$  centered on  $(x_i, y_j)$ .

A box  $X_i \times Y_j$  of  $I$  maps a sine curvature set in parameter space (Fig. 6). It is thus essential to increment accumulators associated with all boxes that intersect at

<sup>1</sup> Finite disjoint union of fuzzy boxes.

least one sine curvature of this set in a non-null manner. This is termed the distributed vote (Fig. 6).

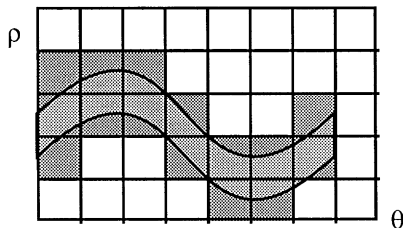


Fig. 6. Sine curves fitted to an image box  $X_i \times Y_j$ .

A first-order approximation can simplify this intersection calculation. Hence, for each  $\theta_q$  value, we evaluate the interval  $[\rho - \Delta\rho, \rho + \Delta\rho]$ , such that

$$\rho = (x_i \cos \theta_q + y_j \sin \theta_q) \quad \text{and}$$

$$\Delta\rho = |\partial x \cos \theta_q| + |\partial y \sin \theta_q| + |(y_j \cos \theta_q - x_i \sin \theta_q) \partial \theta|.$$

The  $P_p \times \Theta_q$  cell accumulator is then incremented, for which

$$[\rho - \Delta\rho, \rho + \Delta\rho] \cap [\rho_p - \partial\rho, \rho_p + \partial\rho] \neq \emptyset. \quad (2)$$

Eq. (2) states that  $(x, y, \rho, \theta) \in X_i \times Y_j \times P_p \times \Theta_q$  exists, such that  $\rho = (x \cos \theta + y \sin \theta)$ , indicating that the relation  $f(x, y, \rho, \theta) = 0$  is entirely possible in this box.

The all-or-none aspect of this incrementation can be astutely reduced by incrementing the accumulator associated with the  $P_p \times \Theta_q$  cell using a proportional value, whereby the  $[\rho - \Delta\rho, \rho + \Delta\rho]$  interval overlaps each  $P_p$  interval. The fuzzy Hough transform formalizes this heuristic process.

4.2.3. Fuzzy vote

Let us consider that each pixel  $(i, j)$  is a fuzzy box, i.e., a product of two fuzzy intervals  $X_i$  and  $Y_j$ .  $X_i$  (rsp.  $Y_j$ ) is a symmetrical fuzzy interval centered on  $x_i$  (rsp.  $y_j$ ) with kernel  $[x_i - \partial x, x_i + \partial x]$  (rsp.  $[y_j - \partial y, y_j + \partial y]$ ) and spread  $\sigma_x$  (rsp.  $\sigma_y$ ) (Fig. 7).

Therefore, the sine curve set produced by each pixel in  $\Omega$  is an induced fuzzy set (Fig. 8).

Each  $\Omega$  cell is stated in the same manner as the Cartesian (fuzzy) product of two fuzzy intervals  $P_p$  and  $\Theta_q$ .  $P_p$  (rsp.  $\Theta_q$ ) is the fuzzy interval with a kernel  $[\rho_p - \partial\rho, \rho_p + \partial\rho]$  (rsp.  $[\theta_q - \partial\theta, \theta_q + \partial\theta]$ ), and spread  $\sigma_\rho$  (rsp.  $\sigma_\theta$ ).

We find that, for each  $X_i \times Y_j$  box of  $E$ , the relation  $f(x, y, \rho, \theta) = 0$  is possible for  $P_p \times \Theta_q$  cells with incremented accumulators. This potential is shown by the fact that the value 0 belongs to the variation domain of  $\phi = f(x, y, \rho, \theta)$  when variables  $x, y, \rho$  and  $\theta$  are restricted by their variation domain.

Variation domains in the FHT are fuzzy. Hence, when  $(x, y, \rho, \theta)$  belongs to  $X_i \times Y_j \times P_p \times \Theta_q$ , the range of the variable  $\phi$  is the fuzzy variation domain  $\Phi_{ijpq}$ . According to the extension principle, when  $\mu_{\Phi_{ijpq}}$  is the membership

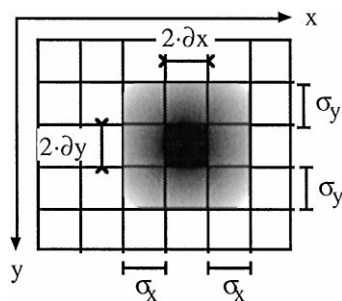


Fig. 7. Fuzzy pixel (fuzzy image box).

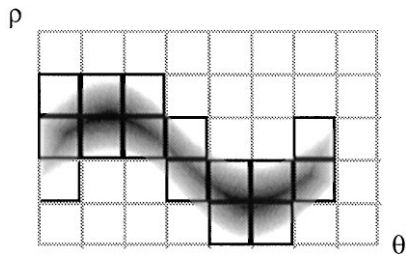


Fig. 8. Fuzzy sine curve set fitted to a fuzzy image box  $X_i \times Y_j$ .

function of  $\Phi_{ijpq}$ , we can state

$$\mu_{\Phi_{ijpq}}(\phi) = \text{SUP}_{\substack{x \in X_i, y \in Y_j \\ \rho \in P_p, \theta \in \Theta_q}} \{ \text{MIN}[\mu_{X_i}(x), \mu_{Y_j}(y), \mu_{P_p}(\rho), \mu_{\Theta_q}(\theta)] / f(x, y, \rho, \Theta) = \phi \}.$$

The possibility of membership of a pixel  $(i, j)$  to the fuzzy line represented by the cell  $(p, q)$  is clearly membership of the value 0 to the fuzzy set  $\Phi_{ijpq}$ :

$$\pi(i, j, p, q) = \mu_{\Phi_{ijpq}}(0)$$

FHT assessment of the fuzzy cell  $P_p \times \Theta_q$  is then defined, for all fuzzy pixels of  $E$ , as the sum of this occurrence possibility  $\pi(i, j, p, q)$ . Replacing the fuzzy boxes by crisp boxes will clearly lead to a classical HT.

Now, to evaluate  $\mu_{\Phi_{ijpq}}(\phi)$ , we will use the properties of fuzzy intervals in an LR representation. The fuzzy intervals used here are for obvious reasons considered to be symmetrical. According to the properties of fuzzy intervals, the fuzzy interval  $\Phi_{ijpq}$  can be defined by

$$\Phi_{ijpq} = P_p - X_i \cdot \cos \Theta_q - Y_j \cdot \sin \Theta_q.$$

Taking into account a few restrictions specific to limited developments,  $\Phi_{ijpq}$  can be mapped with an LR-type interval, as defined by its center  $\phi_{ijpq}$ , the half-width of its kernel  $\partial\phi_{ijpq}$  and its spread  $\sigma_{\Phi_{ijpq}}$ :

$$\phi_{ijpq} \approx f(x_i, y_j, \rho_p, \theta_q) = \rho_p - x_i \cdot \cos \theta_q - y_j \cdot \sin \theta_q,$$

$$\partial\phi_{ijpq} \approx \partial\rho + |\cos \theta_q| \cdot \partial x + |\sin \theta_q| \cdot \partial y + |x_i \sin \theta_q - y_j \cos \theta_q| \cdot \partial\theta,$$

$$\sigma_{\Phi_{ijpq}} \approx \sigma_\rho + |\cos \theta_q| \cdot \sigma_x + |\sin \theta_q| \cdot \sigma_y + |x_i \sin \theta_q - y_j \cos \theta_q| \cdot \sigma_\theta.$$

The FHT assesses the cell  $\{p, q\}$  as follows:

$$\mathcal{H}(P_p \times \Theta_q) = \sum_{X_i \times Y_j \in E} \mu_{\Phi_{ijpq}}(0) = \sum_{X_i \times Y_j \in E} \pi(i, j, p, q).$$

The latter equation still has to be corrected to account for the fact that  $E$  is a fuzzy set of  $I$  with a membership function  $\mu_E(X_i \times Y_j)$ :

$$\mathcal{H}(P_p \times \Theta_q) = \sum_{ij} \text{MIN}(\pi(i, j, p, q), \mu_E(X_i \times Y_j)).$$

HT programming can be substantially simplified if we consider that, for constant  $X_i, Y_j, P_p$  and  $\Theta_q$ , detecting membership of 0 to the fuzzy interval  $\Phi_{ijpq}$  is the same as detecting membership of  $\rho_p$  to the fuzzy set  $P_{ijq}$  whose membership function is that of  $\Phi_{ijpq}$  translated from  $(x_i \cdot \cos \theta_q + y_j \cdot \sin \theta_q) = \rho_{ijq}$  (Fig. 9).

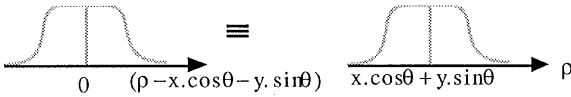


Fig. 9. Pixel-induced fuzzy subset.

HT assessment with  $\Omega$  therefore becomes:

```

FOR EACH IMAGE PIXEL (i, j)
  FOR EACH FUZZY INTERVAL  $\Theta_q$ 
    CALCULATE THE FUZZY SUBSET  $P_{ijq}$ 
    INCREMENT EACH CELL (p, q)
    OF THE QUANTITY
     $\pi(i, j, p, q) = \text{MIN}(\mu_{P_{ijq}}(\rho_p), \mu_E(X_i \times Y_j))$ 
  END FOR
END FOR
    
```

Calculation can be speeded up by checking, before each possibility analysis, whether  $\rho_p$  belongs to  $S(P_{ijq})$ , the support of  $P_{ijq}$ .

### 4.3. Transform interpretation

#### 4.3.1. Peak detection

The constructed HT accumulator array  $\mathcal{H}$  has to be analyzed in order to extract peaks that indicate the presence of straight lines in the image.

Conventional analysis involves setting a threshold at the least number of points required for a definite straight line to appear in the image. The set  $W \subset \Omega$  of chosen cells is obtained by thresholding  $\mathcal{H}$ .

Many studies have shown that a noisy original image, or defects in the technique for selecting characteristic points, reduce the robustness of the method. O’Gorman and Sanderson [25] propose to use a method that performs a robust detection with few hypotheses. However, the presence of elongated peaks – that are numerous in HT – causes misdetections.

Uniform noise in the image gives rise to noise peaks in the transform array. The appearance of these peaks alters

line detection or leads to detection of non-existent lines in the image.

To reduce these negative effects, Cohen and Toussaint [22] suggested using a non-uniform threshold proportional to the probability that noise is present in the image. This requires prior information concerning noise distribution in the original image. The detection threshold will be overestimated if little is known about this distribution, thus eliminating short line segments.

Another problem intrinsic to the uncertainty/precision duality then arises from the lack of correspondence between the quantization of  $\Omega$  and the real straight line detection precision in images (“thick” lines). In such cases, each real straight line can map several related cells from the transform array.

The main methods that have been proposed to overcome this problem are multi-scale analysis, peak detection with a suitable convolution mask and other approaches involving consolidation of related cells. By these techniques, only representative values in each group of related cells can be chosen.

Line detection can be improved by using redundancy of local information. Statistical (median, mean, statistical screening, etc.) and heuristical (influence function, etc.) fusion procedures can be used to improve pinpointing of straight lines in the image, but such techniques are usually only empirically warranted.

We propose replacing binary peak detection with a fuzzy detection procedure. The hypothesis that  $W$  is a fuzzy subset can thus be put forward.

We call upon the distributed voting principle to enhance detection in the neighborhood of each cell  $\Omega$  or group of cells. This procedure is known as “defuzzification”.

#### 4.3.2. Fuzzy detection

We now consider  $W$  as a fuzzy set of  $\mathcal{H}$  peaks on  $\Omega$ . Fuzzy detection now involves assessing the membership function  $\mu_w$  of  $W$  on  $\Omega$ .

Membership of a cell  $(p, q)$  to  $W$  is characterized by two properties:

- the accumulator  $\mathcal{H}(P_p \times \Theta_q)$  has a higher value than those of the set of accumulators in the neighborhood of  $(p, q)$ ,
- the peak mid-points of the minimum and maximum curvatures are negative and their absolute values are high.

Two fuzzy subsets  $W1$  and  $W2$  can be defined according to these two vague premises.  $W1$  is a subset of cells of a highly negative curvature.  $W2$  is a subset of cells with a higher value than those of its neighbors.  $W$  is the fuzzy intersection of  $W1$  and  $W2$ .

To determine  $W1$  for each cell  $(p, q)$ , we calculate two curvature indices  $H(p, q)$  and  $K(p, q)$ , the mean curvature

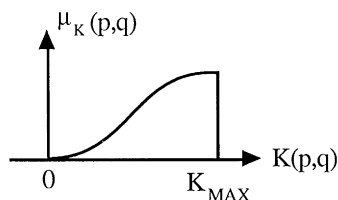


Fig. 10. Membership to sharp curvatures.

and the Gaussian curvature, respectively. A peak is identified when its Gaussian curvature is positive and its mean curvature negative [26]. Membership of a cell  $(p, q)$  to the  $W1$  subset is greatest with a negative  $H(p, q)$  and positive  $K(p, q)$ .

Hence, with an  $\mathcal{L}$ -type function, two fuzzy coefficients  $\mu_H(p, q)$  and  $\mu_K(p, q)$  are obtained by (Fig. 10)

$$\mu_H(p, q) = \mathcal{L}\left(\frac{\text{MIN}(0, H(p, q))}{H_{\text{MIN}}}\right), \quad H_{\text{MIN}} = \text{INF}_{p,q} \{H(p, q)\},$$

$$\mu_K(p, q) = \mathcal{L}\left(\frac{\text{MAX}(0, K(p, q))}{K_{\text{MAX}}}\right), \quad K_{\text{MAX}} = \text{SUP}_{p,q} \{K(p, q)\}.$$

Then  $\mu_{W1}(p, q)$  is defined by:  $\mu_{W1}(p, q) = \mu_H(p, q) \cdot \mu_K(p, q)$ , where “ $\cdot$ ” is a conjunction operator, considering that Gaussian and mean curvatures are computationally linked variables [17].

The fuzzy subset  $W2$  is defined as a fuzzy threshold of the function  $\ell$  on  $\Omega$ . This approach is derived from a classic method, whereby a smoothing filter  $\mathcal{F}$  is passed over an array  $\mathcal{H}$ , and only cells  $(p, q)$  are used, such that  $\ell(P_p \times \Theta_q) - \mathcal{F}(\ell(P_p \times \Theta_q))$  are positive  $\mu_{w2}(p, q)$ , the membership function of  $W2$ , is defined by

$$\mu_{w2}(p, q) = \mathcal{L}\left(\frac{D(p, q)}{D_{\text{MAX}}}\right) \quad (\mathcal{L} \text{ is a form function}),$$

$$D(p, q) = \text{MAX}(0, (\ell(P_p \times \Theta_q) - \mathcal{F}(\ell(P_p \times \Theta_q))))$$

$$D_{\text{MAX}} = \text{SUP}_{p,q} \{D(p, q)\}.$$

Membership of the cell  $(p, q)$  to the  $W$  subset is the defined by

$$\mu_w(p, q) = \mu_{(w1 \cap w2)}(p, q) = \text{MIN}(\mu_{w1}(p, q), \mu_{w2}(p, q)).$$

### 4.3.3. Interpretation

Our goal here is to demonstrate how to obtain information on the real presence of straight lines in an image from the fuzzy subset  $W$ .

According to fuzzy analysis, all straight lines represented by the cells  $(p, q)$  of  $\Omega$  are a priori present in the image but to different degrees. This *degree of presence* or *possibility of presence* is proportional to the membership of the cell  $(p, q)$  in  $W$ .

It would be possible to get this by possibility of presence distribution. However, for most applications, it is

essential to utilize binary information on presence or non-presence. The lines of the crisp subset  $W_\alpha$ , whose possibilities of presence are at least  $\alpha$ , thus have to be deduced from  $W$ . This subset is the  $\alpha$ -cut of  $W$ . An analysis of  $W$  can be carried out to find the *best* cut (according to a specific criterion). In practice, the closest crisp subset is chosen, i.e., the  $(\frac{1}{2})$ -level cut.

### 4.3.4. Defuzzification

In the CHT, the value of the assessment  $\ell$  of the cell  $(p, q)$  relative to the array  $\mathcal{H}$  can be used as a confidence index characterizing the presence of one line of the cell  $P_p \times \Theta_q$  in the real image. This confidence is derived from the number of  $E$  points that have voted for one line of the cell  $P_p \times \Theta_q$ .

Conversely,  $\ell(P_p \times \Theta_q)$  provides no information on the most likely value of  $(\rho, \theta)$  of the cell  $P_p \times \Theta_q$ . The precision in detecting the value of  $(\rho, \theta)$  depends on the quantization of  $\Omega$  only.

In the FHT, on the other hand, precision in detecting the most likely value of  $(\rho, \theta)$  is only partially related to the quantization of  $\Omega$  because of distributed voting. If the quantization is suitable for obtaining clear separation of straight lines on the image, then increasing or decreasing this interval will have little effect on the results.

Indeed, in the FHT, several  $\Omega$  cells can map a real straight line on the original image. The value  $\ell$  in each cell corresponds to the compatibility of a real straight line with the (fuzzy) subset of straight lines represented by this cell.

The method used for assessing the most likely line draws from *defuzzification* principles used in fuzzy control. It involves retrieving the distributed vote for a line of the cell  $(p, q)$  from the neighboring cells by calculating the barycenter of the concerned fuzzy subsets [27].

We explain this process for one-dimensional situations, and our argument is based solely on  $\rho$  (Fig. 11).

$\mu_\rho(\rho_i)$  is the confidence value for a straight line mapped by the  $P_i$  cell. For  $\mu_\rho$ , we can use the normalized value of  $\ell$  on  $\Omega$ :

$$\mu_\rho(\rho_i) = \frac{\ell(\rho_i) - \text{MIN}_k(\ell(P_k))}{\text{MAX}_k(\ell(P_k) - \text{MIN}_k(\ell(P_k)))}.$$

Assuming that information on the real value of  $\rho$  can be extracted from the two neighbors of the  $P_i$  cell, then the  $\hat{\rho}$  value with the best consensus (in terms of the barycenter) is such that

$$\hat{\rho} = \frac{\int r \mu_R(r) dr}{\int \mu_R(r) dr}.$$

$R_i$  is the fuzzy subset whose membership function is defined by

$$\mu_{R_i}(\rho) = \text{SUP}_{k=i-1}^{i+1} (\text{MIN}(\mu_\rho(\rho_k), \mu_{P_i}(\rho_i))).$$



Fig. 11. Defuzzification of the FHT.

From this explanatory formulation, we can easily extract the two-dimensional case by replacing  $\mu_A(\rho_i)$  by  $\mu_A(\rho_i, \theta_j)$  and  $\mu_{R_i}(\rho)$  by  $\mu_{R_i \times Q_j^{(\rho, \theta)}}$ .

4.3.5. Fusion

In Section 4.2, we illustrated that when there is a defect in the starting image (fuzzy, poor contrast, etc.), or when quantization of  $\Omega$  is not suitable for all lines in the original image (it never is), then a real straight line corresponds to a set of  $\Omega$  cells.

It is thus necessary to consolidate the set of cells that surpass the chosen confidence threshold into a set of related cells. Each group of related cells in the accumulator array maps and approximate straight line in the real image. This duplication of information can thus be used to obtain a better estimate of the  $\rho$  and  $\theta$  parameters that best represent a real straight line on the image.

For the CHT, the most robust procedure for determining the best candidate involves choosing the one that has obtained the most votes from the group of related cells.

For the FHT, the neighborhood used in the defuzzification process can be extended to the concerned cell set and fusion can be weighted by the membership function  $\mu_{\ell}$ .

We tested an analogous procedure with the CHT; a mean of related cells is calculated, with each cell weighted with each of its values  $\ell$ . However, the procedure was found to be relatively non-robust since in some cases line detection was degraded by fusion. This problem can be readily explained by the fact that the value  $\ell$  in a cell  $(p, q)$  represents a confidence measurement for the appearance of a set of lines on the image. The values  $\ell$  for neighboring cells of  $(p, q)$  do not contain any information on the appearance of straight lines for  $(p, q)$ . Mean weighted fusion involves scanning a set of related cells for the best parameter value. This assumes that the confidence measurement provided by  $\ell$  is distributed throughout these cells, whereas it is actually located in each box.

5. Experiments

We investigated the fuzzy Hough transform to analyze different grey-level images with various types of noise (fuzzy, unclear lines, grainy and non-uniform backgrounds, poor contrast, etc.). It was found that one of the



Fig. 12. Original image of three cables.

main advantages of the FHT over the CHT is a marked increase in robustness relative to all of the specific parameters required to conduct an Hough Transform (thresholds, quantization, neighbor detection and fusion).

We will now give a few examples comparing straight line seeking using the FHT and CHT. These comparative tests were carried out on a  $512 \times 512$  pixel image with 256 grey levels. This image shows three black cables against a white textured, grainy and irregularly-lit background (Fig. 12).

This example is taken not to *prove* the validity of FHT versus CHT but to illustrate the differences between those methods. In fact, experiments have been run on numerous examples. The setting was chosen because it includes almost all of the following defects:

- uniform noise due to the background texture,
- non-uniform noise due to the lighting,
- poor correspondence of the line model due to the unstraight cables,
- unclear grey-level threshold due to shading.

We tried to match each cable with a line passing as close as possible through its hypothetical center. In this

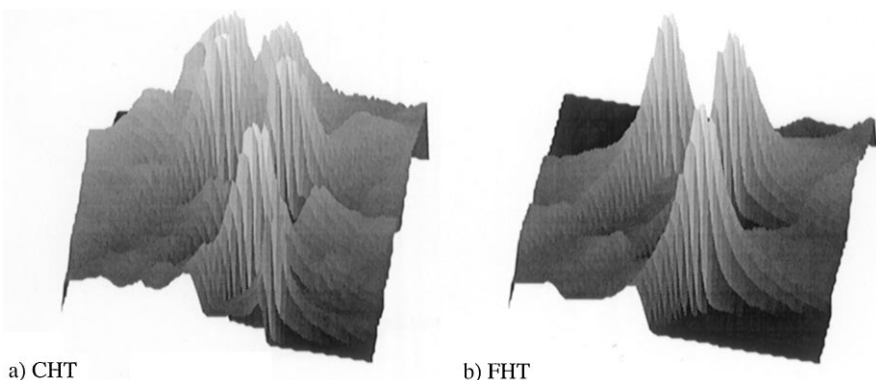


Fig. 13. Accumulator arrays for the CHT (a) and the FHT (b).

example, we highlight the robust qualities of the FHT concerning quantization, thresholding, noise and goodness-of-fit of our line model.

In these comparative tests, we used the same set of parameters for all transforms so as to clearly highlight specific FHT characteristics. For instance, the same grey-level threshold was used in all cases, which served as the non-membership threshold ( $s^-$ ) for the FHT. This meant that  $E_1$ , the kernel of the fuzzy subset  $E$ , was taken as being empty.

Fig. 13 shows the CHT (a) and FHT (b) accumulator arrays for this image. The grey-level threshold and  $\Omega$  quantization were chosen in order to obtain clear cable detection (threshold 20,  $\Omega$ -quantization  $200 \times 200$ ).

There are very few noise peaks in the accumulator array for the FHT, in contrast to that of the CHT. This could be explained by joint effects of a distributed vote and fuzzy weighting, thus “smoothing” the transform.

These two accumulator arrays have the same thresholding (binary) with a relative threshold corresponding to a percentage of the highest peak, designed to eliminate all secondary peaks in the CHT accumulator array. On the original image, we overlaid representative straight lines from the centers of each cell (Fig. 14).

In both cases, the detected lines closely matched real lines passing through all or part of the set of points for each cable. The only noteworthy difference is the high number of diagonal lines retained by the THC. This difference can be explained by texture-induced noise in the extraction of characteristic image points during thresholding.

We then applied HT-specific fusion methods, i.e., peak detection (CHT) and defuzzification (FHT). Despite a suitable grey-level threshold choice, the combined texture/non-uniform lighting induced noise peaks on the CHT. We thus chose an accumulator array binarization threshold that would eliminate any possible appearance of these peaks. However, the background noise biased detection with the CHT (Fig. 15 (a)), while it had no visible effect on the FHT (Fig. 15 (b)).

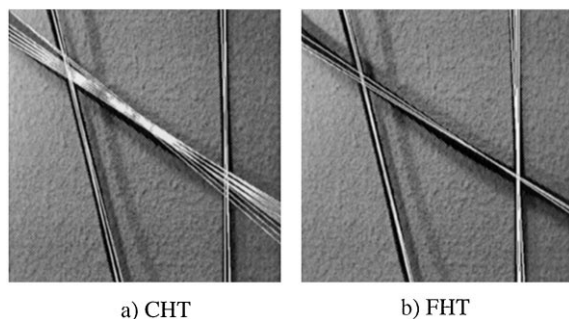


Fig. 14. Detected straight lines superimposed on the original image.

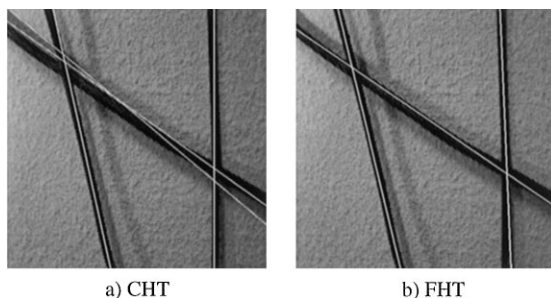


Fig. 15. Line detection after fusion.

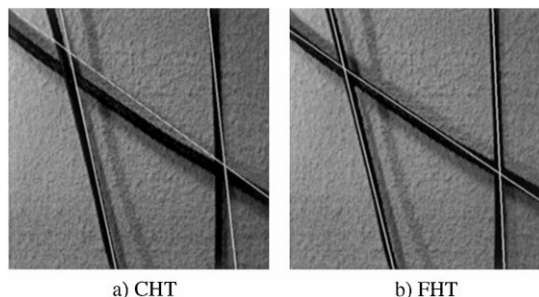


Fig. 16. Poor quantization of  $\Omega$ .

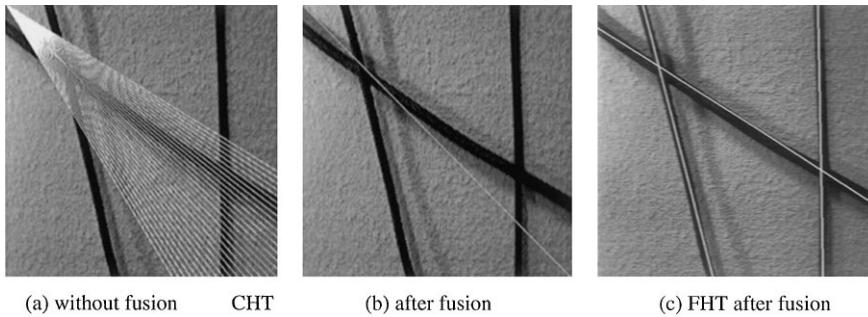


Fig. 17. Poor grey-level threshold.

For the CHT, line detection precision decreased when the number of cells covering  $\Omega$  was reduced. For the FHT, when the sample was large enough to obtain good cell separation, reduced quantization had little effect on the results. Fig. 16 (a) and (b) compares the behaviors of the THF and the THC for quantization of  $\Omega$  in  $40 \times 40$  cells at the same threshold (20).

Finally, for the CHT, background noise had a clear overriding effect when the grey-level threshold chosen to define the subset  $E$  of characteristic points was not correct (Fig. 17 (a) and (c)). In contrast, for the FHT, the poorly defined threshold had almost no effect on line detection precision (Fig. 17(b)).

Overall, the results of these tests showed that when the analyzed image is crisp, well contrasted, with little noise and quantization is adequate, then there is no visible improvement in the quality of straight line detection on the image when using the FHT. However, in the absence of any of these characteristics, there is clear detection degradation with the CHT but not with the FHT. The FHT is therefore more robust than the CHT.

## 6. Conclusion and discussion

The Hough transform (HT) is a popular technique for detecting parametric forms such as straight lines in images. However, it is somewhat difficult to set up since several parameters must first be defined, e.g. quantization thresholds and intervals. Noisy original images can bias or even hinder detection. Finally, there is also another real problem, which we have termed the uncertainty/precision duality, stated as follows: as detection precision increases, confidence in the detection decreases.

The fuzzy Hough transform (FHT) is a new formulation of the classical Hough transform (CHT) which draws from fuzzy subset theory. There are three major modifications to the classical theory:

- definition of a subset of characteristic image points,
- quantization of the domain and range,
- transform interpretation.

These modifications enhance accumulation processes, upon which the transform is based, and disassociate detection precision and parametric space quantization.

Finally, the main feature of the FHT is that threshold and quantization definitions have little effect on its results. We can thus state that it is more *robust* than the CHT.

The obvious drawback of this robustness is the marked increase in computation time, which can be readily overcome by reducing parametric space quantization. Such reductions do not degrade detection precision or the robust properties of the FHT. However, it decreases its ability to discern two close lines.

Furthermore, images with many objects, or edges which are closely parallel, cause confusion in the lines found by both CHT and FHT. But this problem was not addressed here and robust solutions have been proposed (see e.g. [28]).

We specifically focused on straight line detection in images in the present article. Our technique could easily be extended to detection of other more complex parametric forms such as second-degree curves. It can also be improved.

The technique could be further improved in several ways, in particular with respect to the transform interpretation process. For instance, (fuzzy) segmentation of the subset of characteristic points could be used as an alternative to the defuzzification procedure proposed here. Multi-scale analysis could also be used to dissociate detection precision and confidence information contained in the FHT. Finally, a dual transform (contrary to that proposed here) could be designed, whereby points of the  $E$ -complement set would vote so that a necessity array associated with fuzzy boxes of  $\Omega$  could be constructed. Then a process very close to the suboptimal method proposed by [8] could be used. It would consist of detecting peaks no longer in the FHT accumulator but in the “test hypothesis” accumulator given by division of the possibility array and the necessity array. This would lead to an improvement of the ability of the Hough transform to identify very short lines. This would completely separate precision and certainty.

## References

- [1] P. Hough, Method and means for recognizing complex pattern, U.S. Patent no. 3,069,654, December 1962.
- [2] A. Rosenfeld, *Picture Processing by Computer*, Academic Press, New York, 1969.
- [3] R. Duda, P. Hart, Use of the Hough transform to detect lines and curves in pictures, *Commun. ACM* 15 (1972) 11–15.
- [4] D. Shapiro, Transformation for the computer detection of curves in noisy pictures, *Comput. Graphics Image Process* 4 (1975) 328–338.
- [5] G. Gerig, Linking image space and accumulator space: a new approach for object recognition, in: *First International Conference on Computer Vision London*, June 1987, pp. 112–117.
- [6] H. Li, M. Lavin, R. LeMaster, Fast Hough transform: a hierarchical approach, *CVGIP* 36 (1987) 139–161.
- [7] J. Illingworth, J. Kittler, The adaptive Hough transform, *IEEE Trans. PAMI* 9 (1987) 690–698.
- [8] J. Princen, J. Illingworth, J. Kittler, Hypothesis testing: a framework for analysing and optimizing Hough transform performance, *IEEE Trans. PAMI* (4) (1994) 329–341.
- [9] H. Maître, Un panorama de la transformation de Hough, *Trait. Signal* 2 (4) (1985).
- [10] J. Illingworth, J. Kittler, A survey of the Hough transform, *Comput. Vision Graphics Image Process.* 44 (1988) 87–116.
- [11] P. Picton, Hough transform references, *Int. J. Pattern Recognition Artif. Intell.* 1 (1987) 413–425.
- [12] V. Leavers, Which Hough transform, *CVGIP: Image Understanding* (2) (1993) 250–264.
- [13] H. Kälviäinen, P. Hirvonen, L. Xu, E. Oja, Probabilistic and non-probabilistic Hough transforms: overview and comparisons, *Image Vision Comput.* (4) (1995) 239–252.
- [14] J.H. Han, L.T KÓczy, T. Poston, Fuzzy Hough transform, in: *Second International Conference on Fuzzy Systems*, San Francisco, March 1993.
- [15] P. Thrift, S. Dunn, Approximating point-set images by line segments using a variation of the Hough transform, *Comput. Vision Graphics Image Process.* 21 (1983) 383–394.
- [16] A. Kaufmann, *Introduction à la théorie des sous-ensembles flous*, Masson, Paris, 1973.
- [17] D. Dubois, H. Prade, *Possibility Theory: An Approach to Computerized Processing of Uncertainty*, Plenum Press, New York, 1988.
- [18] J. Jolion, A. Rozenfeld, A  $O(\log n)$  pyramid Hough transform, *Pattern Recognition Lett.* 9 (1989) 343–349.
- [19] F. O’Gorman, M. Clowes, Finding picture edges through collinearity of feature points, in: *Third International Joint Conference on Artificial Intelligence*, Stanford August 1973, pp. 543–555.
- [20] T. Wonnacott, *Introductory Statistics for Business and Economics*, Wiley, New York, 1990.
- [21] T. Van Veen, F. Grøen, Discretization errors in the Hough transform, *Pattern Recognition* 14 (1981) 137–145.
- [22] M. Cohen, G. Toussaint, On the detection of structures in noisy pictures, *Pattern Recognition* 9 (1977) 95–98.
- [23] J. O’Rourke, K. Sloan, Dynamic quantization: two adaptive data structures for multidimensional space, *IEEE Trans. PAMI* (3) (1984) 266–288.
- [24] J.M. Chassery, A. Montanvert, *Géométrie discrète en analyse d’images*, Hermes, 1991.
- [25] F. O’Gorman, A.C. Sanderson, The converging squares algorithm: an efficient method for locating peaks in multidimensions, *IEEE Trans. PAMI* (3) (1984) 280–288.
- [26] P. Besl, R. Jain, Segmentation through symbolic surface description, *IEEE Comput. Vision Pattern Recognition* (1986) 77–85.
- [27] L. Foulloy, S. Galchet, *Contrôleur flous: représentation, équivalences et études comparatives*, Rapport LAMII 92-4, juillet 1992.
- [28] P. Palmer, M. Petrou, J. Kittler, A Hough transform with a 2D hypothesis testing kernel, *CVGIP: Image Understanding* (2) (1993) 221–234.

**About the Author**—OLIVIER STRAUSS was born in Dijon, France in 1963. He received his Ph.D. in 1992 from the University of Montpellier. Dr. Strauss has been Associate Professor of Robotics at the University of Montpellier from 1992. His current research interests include error in signal, sensor fusion, vision and image analysis.